ChemPubSoc Europe
DOI: 10.1002/cctc.201501219
CHEMCATCHEM
Communications

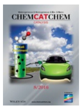

A Facile and Efficient Modification of CNTs for Improved Fischer–Tropsch Performance on Iron Catalyst: Alkali Modification

Renjie Liu, Yan Xu, Zhenhua Li,* and Xinbin Ma*[a]

In this paper, a facile and environmentally benign method is used to pretreat carbon nanotubes (CNTs) by alkali modification, which decreases the wall thickness, increases the inner diameter, and improves the graphitization degree of CNTs compared to conventional acid treatment. The iron catalyst supported on alkali modified CNTs shows extraordinary Fischer–Tropsch synthesis (FTS) activity and CO conversion (1.78 and 2.41 times, respectively) compared with those supported on either the acid treated or pristine CNTs. Additionally, the diesel (C_{10-20}) selectivity on Fe/CNTs-Na is up to 60%, which is much higher than that calculated from the Anderson–Schulz–Flory distribution (39%). Similar results are also found by using activated carbon (AC) and N-doped multiwall carbon nanotubes (NCNTs) as supports for FTS, proving the universal applicability of alkali modification on carbon material. The positive relationship between the C_{5+} selectivity and C_2–C_4 olefin/paraffin ratio of iron catalyst can also be achieved irrespective of the support type.

With increasing resource crisis and stringent environment issues, seeking renewable and sustainable energy resources and developing green technology is the focus point to solve the problem restricting the development of society. Fischer–Tropsch synthesis (FTS) is an alternative non-petroleum route to produce super-clean fuel and build chemicals from the syngas (H_2+CO) derived from coal, biomass, nature gas, or shale gas.[1] High selectivity to desired products is still a challenging problem to avoid extensive recycling of undesired light products to syngas or the subsequent hydrogenation processing of FTS heavy hydrocarbon.[2] According to the Anderson–Schulz–Flory (ASF) distribution of the FTS reaction, the diesel (C_{10-20}) selectivity is limited to 39%. Iron-based catalysts, with the advantages of high activity and low price, have aroused the increasing attention of industrial researchers and academics. The high water-gas-shift (WGS) activity on iron catalyst was beneficial for tuning the H_2/CO ratio of the syngas generated from coal or biomass. For these reasons, a supported iron catalyst is considered as one of the most promising catalysts for FTS process.[3] In addition, the support property could affect the dispersion, distribution, reduction, carbonization, and then the catalytic performance (activity and selectivity) of the supported iron catalyst. Compared with conventional oxide supports, carbon materials are ideal support candidates owing to their unique properties, such as an inert surface, high electronic conductivity, high mechanical and chemical stability, as well as well-refined nanochannel structure.[4] The flexibility of tuning the physicochemical properties of carbon materials makes research of the intrinsic catalytic mechanism particularly interesting. Acid treatment is widely used to functionalize carbon nanotubes (CNTs), but this procedure is detrimental to the environment. To date there are limited reports of using alkali treatment on CNTs was reported.[5]

Here, we report a facile and environmental benign method to modify CNTs by alkali treatment (see the Supporting Information for more details) with a high degree of graphitization and a large inner diameter. The modified material was subsequently used as a support for an iron-based catalyst, which was applied to the FTS reaction. The CNTs-t represents the CNTs after nitric acid treatment.[6] As seen in Figure 1, CNTs-Na (Figure 1c) shows a larger inner diameter than pristine CNTs (Figure 1a) and CNTs-t (Figure 1b). The distribution bar graph of inner/outer diameters for the pristine CNTs and treated CNTs have been shown in Figure S1 (Supporting Information). Notably, the tube wall thickness of CNTs-Na decreases compared with pristine CNTs and CNTs-t. Both pristine CNTs and CNTs-Na display more or less closed caps, but no closed caps are found for CNTs-t. Clearly, the treatment CNTs with acid and alkali results in different mechanisms. As reported previously, the acid treatment of CNTs could introduce more oxygen-containing groups, remove the amorphous carbon and metallic impurities and open the caps.[7] However, the alkali modification may lead to not only the amorphous carbon removed, but also the graphite layer of the CNTs exfoliated.

Thermogravimetric (TG) analysis of the supports and the corresponding catalysts were performed to study the influence of treatment methods and iron loading on the thermal stability of CNTs (Figure 2). Clearly, the initial temperature of CNTs-t is lower than those of the other samples, owing to the presence of oxygen-containing functional groups in the tube surface.[8] Higher O content in CNTs-t from the XPS result (Table S1, Supporting Information) also reflects the more oxygen-containing functional groups, which implies more defects or structural damages were produced along the tubes. It was reported that

---

[a] Dr. R. Liu, Assoc. Prof. Dr. Y. Xu, Prof. Dr. Z. Li, Prof. Dr. X. Ma
Key Lab for Green Chemical Technology of Ministry of Education
Collaborative Innovation Center of
Chemical Science and Engineering
School of Chemical Engineering and Technology
Tianjin University
Tianjin 300072 (P.R. China)
E-mail: zhenhua@tju.edu.cn
xbma@tju.edu.cn

Supporting information for this article is available on the WWW under http://dx.doi.org/10.1002/cctc.201501219.

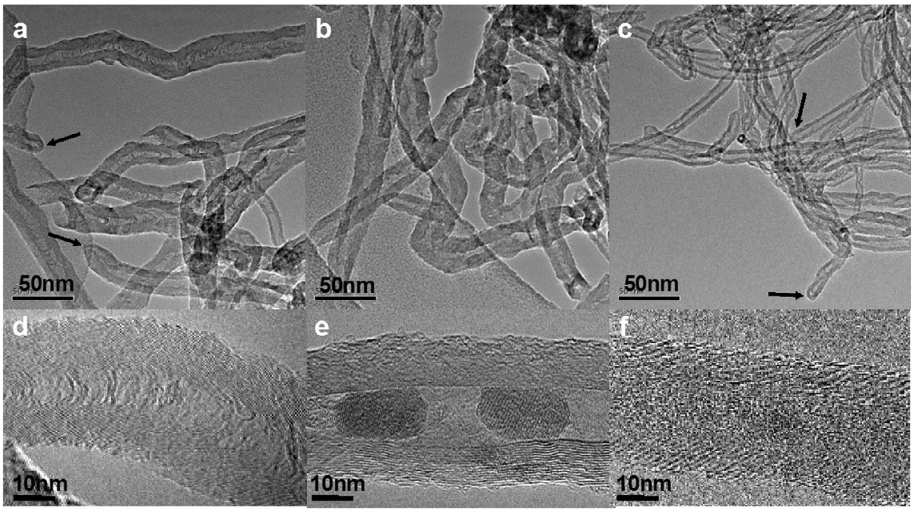

Figure 1. Representative TEM images of pristine a) CNTs, b) CNTs-t, c) CNTs-Na, as-prepared catalysts d) Fe/CNTs, e) Fe/CNTs-t, and Fe/CNTs-Na. Arrowed lines indicate the closed caps.

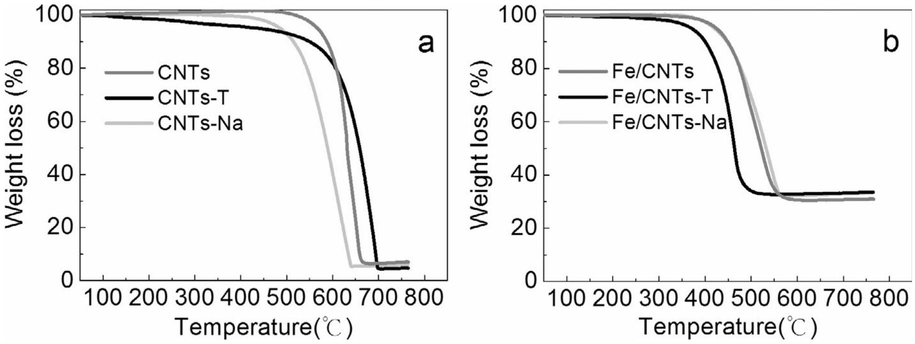

Figure 2. TG profiles of the supports (a) and the corresponding catalysts after calcinations (b).

the defects and open caps contributed to high dispersion of iron particles throughout the CNTs tubes, which was also confirmed by TEM results (Figure S3 a).[9] Comparatively, the oxidation temperature of the CNTs-Na is lower than those of the other samples, suggesting that CNTs modified by the alkali are more vulnerable to oxidative destruction, which may be related to the decreased thickness of CNTs indicated by the TEM results (Figure 1 c).[10] A similar result is observed for the alkali modification of other carbon materials, such as activated carbon (AC) and N-doped multiwall carbon nanotubes (NCNTs) (Figure S2). Additionally, the weight of ash residue of CNTs-t above 600 °C decreases more heavily than that of CNTs-Na, which indicates that acid treatment could remove more impurity and amorphous carbon than alkali treatment. However, an shift to low temperature is observed from the stability of iron supported on CNTs, which is attributed to the catalysis effect of iron on the CNTs oxidation.[8,11] The mass of remnants (α-Fe_2O_3) for all the catalysts after calcination is near 27 %, corresponding to 18.9 % Fe, which is close to the theoretical Fe loading 20 wt % on the CNTs.

The Raman spectra of the pristine CNTs, CNTs-t, and CNTs-Na were recorded (Figure 3). The D mode around 1340 cm^{-1} corresponding to the disorder-induced band is an indicative of impurities or other symmetry-breaking defects. The G mode around 1575 cm^{-1}, corresponding to the tangential vibrations of the carbon atoms is related to the ordered graphite in the CNTs.[12] The intensity ratio of the D-band to that of G-band (I_D/I_G) is used to evaluate the graphitization degree of carbon ma-

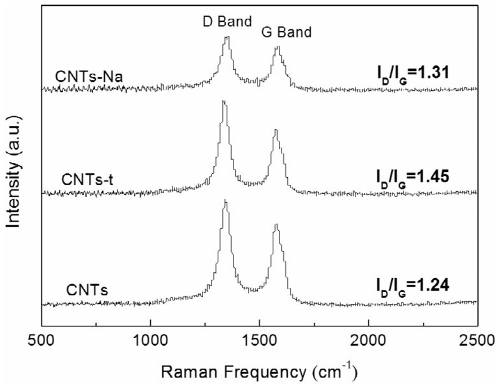

Figure 3. Raman spectra of the CNTs treated by different methods.

terials.[13] As listed in Figure 3, the graphitization degree of CNTs-t is the lowest. Notably, the amorphous carbon can be efficiently removed by acid treatment, which will inevitably introduce more oxygen-containing groups and defects through the tubes.[6] Superposition of these two factors makes the CNTs-t having a lower graphitization degree than the pristine sample. Comparatively, CNTs-Na displays the highest graphitization degree reflected by the I_D/I_G. High graphitization degree of the carbon support facilitates the electron transfer between the active species and CO molecules. The activation of CO might be enhanced, accompanied with an improved FTS reaction activity.[14] Notably, the G-bond intensity of the CNTs is closely diameter dependence of the tube.[15] The G-band intensity of CNTs-Na is the lowest among these samples, which corresponds to the smallest diameter of tubes. This observation is consistence with the TEM and TG analysis (Figure 1 c and Figure 2).

The physical properties of the supports and corresponding catalysts were presented in Table S1. It is clear that either acid or alkali treatment of CNTs increases the specific surface area with bigger increment for CNTs-t. The CNTs-Na displays a bigger average pore size than CNTs-t, which is in agreement with the TEM results (Figure 1 c). Furthermore, both the pore volumes and average pore sizes of the three catalysts decrease compared with the corresponding supports. The representative TEM images of the as-prepared iron catalysts were shown in Figure S3. More endohedral iron particles than the exposed iron particles can be found on Fe/CNTs-t and Fe/CNTs-Na, owing to the open cap and capillary force effect.[16] However, almost no particles are located on the CNTs interior surface for Fe/CNTs. In this study, the carbon material treated by alkali is washed with deionized water until reaching a neutral pH, and no residual Na on the catalyst is detected by EDS or XPS analysis.

According to the XRD results (Figure 4), the peaks at $2\theta = 25.9°$ and 43.0° are assigned to (002) and (100) diffractions of graphitic carbon.[17] Both Fe/CNTs and Fe/CNTs-Na show a mixture of the crystal phase of α-Fe_2O_3 (JCPDS no.33-0664) and Fe_3O_4 (JCPDS no.19-0629), whereas Fe/CNTs-t contains a single Fe_3O_4 crystalline phase, which may be attributed to the different support properties and the location of iron particle. The phase transition from α-Fe_2O_3 to Fe_3O_4 is mainly related to the autoreduction of iron oxides during the calcination in Ar. The iron oxides located inside the tubes or attached on the defect sites of the carbon material can be easily reduced, owing to the weakened metal–oxygen bonding.[18] Additionally, the autoreduction degree is enhanced with the decrease of the inner diameter of CNTs.[19] This also demonstrates that alkali modification could increase the inner diameter of CNTs, which is in good agreement with the above results.

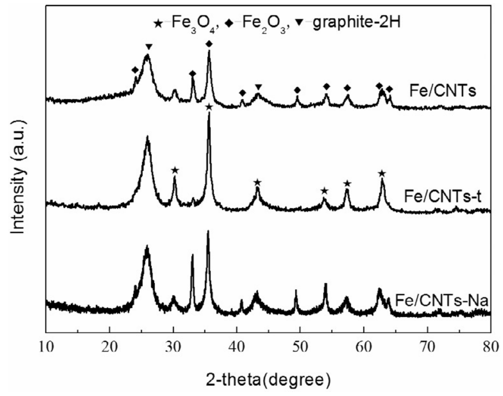

Figure 4. XRD patterns of the as-prepared iron catalysts.

The reduction properties of the as-prepared catalysts were determined by H_2-TPR (Figure S4). All the catalysts exhibit three partly overlapping peaks: the first two peaks around 200–600 °C can be assigned to the reduction of Fe_2O_3 or Fe_3O_4 to metallic Fe with FeO as the intermediate species[20] and the tail peak over 600 °C ascribed to the carbon gasification.[16] The reduction degree of Fe/CNTs-Na is higher than that of Fe/CNTs-t (Table S1). It is reported that iron carbides is active phase for iron-based FTS catalyst[21] and the formation of iron carbides is much related with the reduction degree of iron oxides.[22] So, it is expected that the alkali modification can be an effective route to modify the CNTs for the supported iron-based FTS catalyst.

Figure 5 a shows the variations of CO conversion and C_{5+} selectivity with time on stream (TOS) for three catalysts. The FTS results were summarized in Table 1 by averaging the values from 15 h to 35 h when the reaction was achieved steady-state. At the tested reaction condition, the FTS result on the blank CNTs showed no activity, which indicated that the residual metal on CNTs has no activity toward FTS, whereas CNTs supported Fe catalyst showed significant FTS activity. As listed in Table 1, both the acid and alkali modifications of CNTs can improve the FTS performance of the supported iron catalysts

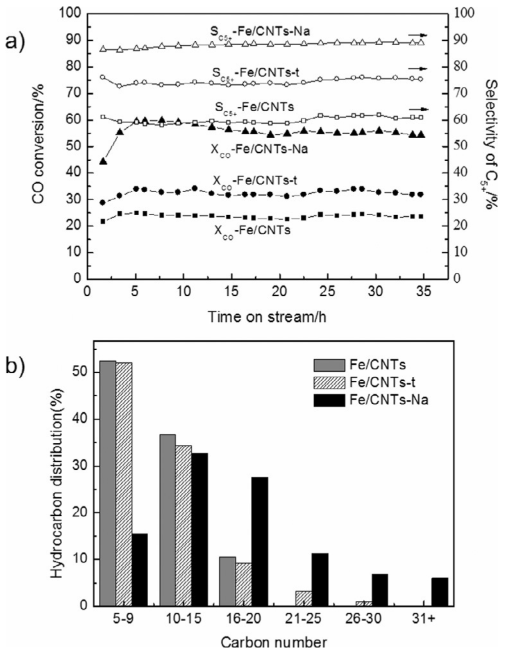

Figure 5. a) CO conversion and C_{5+} selectivity VS time on stream. Reaction conditions: $T = 270$ °C, $P = 2$ MPa, $H_2/CO = 1$ and $WHSV = 4500\ h^{-1}$. b) The C_{5+} hydrocarbon distributions on different catalysts.

Table 1. Activities and hydrocarbon selectivities of different catalysts.[a]

Catalyst	X_{CO} [%]	S_{CO_2} [%]	Hydrocarbon selectivity [%]					$C_=/C_-$[b]
			CH_4	C_2	C_3	C_4	C_5	
Fe/CNTs	23.4	16.1	29.0	6.4	3.8	1.8	59.0	0.09
Fe/CNTs-t	31.6	13.5	16.0	4.3	4.2	2.4	73.0	0.89
Fe/CNTs-Na	56.4	35.5	5.4	2.6	2.3	1.3	88.5	3.83

[a] Reaction conditions: $T = 270\,^{\circ}C$, $P = 2$ MPa, $n(H_2)/n(CO) = 1$ and WHSV = 4500 h^{-1}. [b] Mainly for C_2–C_4 hydrocarbons.

with the Fe/CNTs-Na showing a remarkable increase. The high graphitization degree, high reduction degree and high iron dispersion of Fe/CNTs-Na are responsible for its superior FTS catalytic performance. Additionally, the formation of CH_4 and light hydrocarbons are greatly suppressed for Fe/CNTs-Na, whereas the desired heavy hydrocarbons selectivity increases a lot. The high C_{5+} selectivity (88.5%) may be related to not only the internal location of the active iron phase in CNTs but also the big inner diameter of support, which can benefit for the formation of long chain hydrocarbons.[16,23] The hydrocarbon distributions of different catalysts are shown in Figure 5b. Compared to Fe/CNTs, the Fe/CNTs-t and Fe/CNTs-Na show a trend toward heavy hydrocarbons production. Moreover, high diesel selectivity (about 60%) is achieved over Fe/CNTs-Na, which breaks restriction of the ASF law (39%). Usually, high diesel-fuel selectivity is difficult to achieve over iron catalysts without the use of promoters. To the best of our knowledge, our catalyst displays the highest diesel-fuel selectivity obtained by a non-promoted iron catalyst, which realizes a great potential for a new route to the synthesis of diesel fuel through the FTS process.

Here, both Fe/CNTs-t and Fe/CNTs-Na display good stabilities during 35 h reaction. As reported previously, the aggregation and re-oxidation of active phase were main reasons for the deactivation of the carbon supported Fe catalyst. The Ostwald ripening process can result in the sintering of iron species supported on carbon material.[24] The inside location of active phase in the tube of CNTs can anchor the active phase in stable manner, owing to the confinement effect.[19,23] Fe_3O_4 has been established as the active phase for the WGS reaction.[25] The existence of iron oxides stabilize the supported iron carbides against irreversible deactivation from re-oxidation by regulating the WGS reaction versus FTS.[26] Moreover, Fe/CNTs-Na with the high WGS activity can effectively impede the re-oxidation of iron carbide by the generated water. The XRD patterns of used catalysts were shown in Figure S5. The peaks belonging to the Fe_5C_2 and Fe_3O_4 can be detected for all the spent catalysts. Clearly, Fe/CNTs-Na shows more Fe_5C_2 than the others, corresponding to a greater reduction and carbonization degree and, hence an improved FTS performance.[6]

In addition, the positive relationship between the C_{5+} and C_2–C_4 olefin/paraffin ratio was established (Figure S6). The variation in C_2–C_4 olefin/paraffin ratio may be associated with the olefin hydrogenation activity.[27] The low hydrogenation activity corresponds to a high C_2–C_4 olefin/paraffin ratio. It has been suggested that a high C_2–C_4 olefin/paraffin ratio is beneficial for chain-growth activity and the formation of C_{5+}, which results in increased α-olefin re-adsorption capacity for chain propagation.[28] Therefore, there is a positive correlation between C_{5+} selectivity and the C_2–C_4 olefin/paraffin ratio.

Herein, to explore the universal applicability of the alkali modification on other carbon materials, AC and NCNTs are also treated by above method and the as prepared supporting iron catalysts were tested for FTS. The results confirm that the catalysts supported on alkali modified carbon materials display enhanced FTS activity and C_{5+} selectivity, and that there is a general applicability for the alkali modification of carbon material as expected (Figure S7 and S8).

This report establishes a facile and environmentally benign method for the modification of CNTs by alkali treatment, which can then be employed as supports for an iron-based FTS catalyst. The alkali modification could decrease wall thickness, increase inner diameter, and improve the graphitization degree of CNTs. The Fe/CNTs-Na catalyst displays an excellent FTS performance with high chain-growth probability. An especially high diesel-fuel selectivity is achieved (60%) over Fe/CNTs-Na. The universal applicability of the alkali modification on other carbon materials for supported iron catalyst has also confirmed. We believe that this research will open up a new treatment method for the CNTs functionalization and the diesel-fuel production for industrial applications. In addition, the high WGS activity on Fe/CNTs-Na catalyst makes the alkali modification applicable to a broad range of fuel-processing reactions. Further research continues into the synergistic effect of pore size and graphitization degree of the carbon support of our iron catalysts for FTS.

Experimental Section

The alkali treatment was performed using the hydrothermal method. After the treatment, the suspension is filtered and washed with de-ionized water until a neutral pH is reached, followed by drying at 110 °C overnight. The resulting sample is designated CNTs-Na for further use as an iron catalyst support. The 20 wt% Fe catalyst was prepared by an impregnation method, so are the Fe/CNTs and Fe/CNTs-t. The samples were characterized by N_2 adsorption, transmission electron microscopy, thermal gravimetric analysis, X-ray diffraction, X-ray photoelectron spectroscopy, Raman spectroscopy and H_2 temperature-programmed reduction. More details on the preparation methods, characterization, and activity of these catalysts are provided in the supporting information.

Acknowledgements

We greatly appreciate the financial support from the National Natural Science Foundation of China (U1462204) and Program of Introducing Talents of Discipline to Universities (B06006).

Keywords: carbon · Fischer–Tropsch synthesis · heterogeneous catalysis · iron

[1] a) A. Y. Khodakov, W. Chu, P. Fongarland, *Chem. Rev.* **2007**, *107*, 1692–1744; b) E. de Smit, B. M. Weckhuysen, *Chem. Soc. Rev.* **2008**, *37*, 2758–2781.

[2] a) J. Kang, K. Cheng, L. Zhang, Q. Zhang, J. Ding, W. Hua, Y. Lou, Q. Zhai, Y. Wang, *Angew. Chem. Int. Ed.* **2011**, *50*, 5200 – 5203; *Angew. Chem.* **2011**, *123*, 5306 – 5309; b) X. Peng, K. Cheng, J. Kang, B. Gu, X. Yu, Q. Zhang, Y. Wang, *Angew. Chem. Int. Ed.* **2015**, *54*, 4553 – 4556; *Angew. Chem.* **2015**, *127*, 4636 – 4639.

[3] M. Casavola, J. Hermannsdörfer, N. de Jonge, A. I. Dugulan, K. P. de Jong, *Adv. Funct. Mater.* **2015**, *25*, 5309 – 5319.

[4] a) A. Saha, C. Jiang, A. A. Martí, *Carbon* **2014**, *79*, 1 – 18; b) Y. Yan, J. Miao, Z. Yang, F. X. Xiao, H. B. Yang, B. Liu, Y. Yang, *Chem. Soc. Rev.* **2015**, *44*, 3295 – 3346.

[5] a) M. L. Toebes, J. M. P. van Heeswijk, J. H. Bitter, A. Jos van Dillen, K. P. de Jong, *Carbon* **2004**, *42*, 307 – 315; b) G. Bezemer, A. Van Laak, A. Van Dillen, K. P. de Jong, *Stud. Surf. Sci. Catal.* **2004**, *147*, 259 – 264.

[6] Z. Li, R. Liu, Y. Xu, X. Ma, *Appl. Surf. Sci.* **2015**, *347*, 643 – 650.

[7] H. Liu, T. Ye, C. Mao, *Angew. Chem. Int. Ed.* **2007**, *46*, 6473 – 6475; *Angew. Chem.* **2007**, *119*, 6593 – 6595.

[8] G. S. McKee, K. S. Vecchio, *J. Phys. Chem. B* **2006**, *110*, 1179 – 1186.

[9] a) R. M. Malek Abbaslou, A. Tavasoli, A. K. Dalai, *Appl. Catal. A* **2009**, *355*, 33 – 41; b) T. Fu, R. Liu, J. Lv, Z. Li, *Fuel Process. Technol.* **2014**, *122*, 49 – 57.

[10] D. K. Singh, P. K. Iyer, P. K. Giri, *J. Appl. Phys.* **2010**, *108*, 084313.

[11] H. Xiong, M. Moyo, M. A. Motchelaho, Z. N. Tetana, S. M. A. Dube, L. L. Jewell, N. J. Coville, *J. Catal.* **2014**, *311*, 80 – 87.

[12] D. Baskaran, J. W. Mays, M. S. Bratcher, *Angew. Chem. Int. Ed.* **2004**, *43*, 2138 – 2142; *Angew. Chem.* **2004**, *116*, 2190 – 2194.

[13] a) M. S. Strano, C. A. Dyke, M. L. Usrey, P. W. Barone, M. J. Allen, H. Shan, C. Kittrell, R. H. Hauge, J. M. Tour, R. E. Smalley, *Science* **2003**, *301*, 1519 – 1522; b) K. Zhang, Q. Zhao, Z. Tao, J. Chen, *Nano Res.* **2013**, *6*, 38 – 46.

[14] J. Xiao, X. Pan, S. Guo, P. Ren, X. Bao, *J. Am. Chem. Soc.* **2015**, *137*, 477 – 482.

[15] A. Jorio, M. A. Pimenta, A. G. Souza Filho, G. G. Samsonidze, A. K. Swan, M. S. Ünlü, B. B. Goldberg, R. Saito, G. Dresselhaus, M. S. Dresselhaus, *Phys. Rev. Lett.* **2003**, *90*, 107403.

[16] R. M. M. Abbaslou, A. Tavassoli, J. Soltan, A. K. Dalai, *Appl. Catal. A* **2009**, *367*, 47 – 52.

[17] J. Jang, J. H. Oh, G. D. Stucky, *Angew. Chem. Int. Ed.* **2002**, *41*, 4016 – 4019; *Angew. Chem.* **2002**, *114*, 4188 – 4191.

[18] W. Chen, X. Pan, M. G. Willinger, D. S. Su, X. Bao, *J. Am. Chem. Soc.* **2006**, *128*, 3136 – 3137.

[19] W. Chen, X. Pan, X. Bao, *J. Am. Chem. Soc.* **2007**, *129*, 7421 – 7426.

[20] R. M. M. Abbaslou, J. Soltan, A. K. Dalai, *Appl. Catal. A* **2010**, *379*, 129 – 134.

[21] C. Yang, H. Zhao, Y. Hou, D. Ma, *J. Am. Chem. Soc.* **2012**, *134*, 15814 – 15821.

[22] S. H. Kang, H. M. Koo, A. R. Kim, D. H. Lee, J. H. Ryu, Y. D. Yoo, J. W. Bae, *Fuel Process. Technol.* **2013**, *109*, 141 – 149.

[23] W. Chen, Z. L. Fan, X. L. Pan, X. H. Bao, *J. Am. Chem. Soc.* **2008**, *130*, 9414 – 9419.

[24] S. H. Joo, S. J. Choi, I. Oh, J. Kwak, Z. Liu, O. Terasaki, R. Ryoo, *Nature* **2001**, *412*, 169 – 172.

[25] G. P. Van Der Laan, A. A. C. M. Beenackers, *Catal. Rev.* **1999**, *41*, 255 – 318.

[26] P. Thüne, P. Moodley, F. Scheijen, H. Fredriksson, R. Lancee, J. Kropf, J. Miller, J. W. Niemantsverdriet, *J. Phys. Chem. C* **2012**, *116*, 7367 – 7373.

[27] E. Iglesia, S. C. Reyes, R. J. Madon, S. L. Soled, *Adv. Catal.* **1993**, *39*, 221 – 302.

[28] R. J. Madon, E. Iglesia, *J. Catal.* **1993**, *139*, 576 – 590.

Received: November 5, 2015